Published in final edited form as:
J Mol Cell Cardiol. 2013 October ; 63: . doi:10.1016/j.yjmcc.2013.07.014.

Coronary adventitial cells are linked to perivascular cardiac fibrosis via TGFβ1 signaling in the *mdx* mouse model of Duchenne Muscular Dystrophy

Nicholas Ieronimakis[1], **Aislinn L. Hays**[1], **Kajohnkiart Janebodin**[2], **William M. Mahoney Jr.**[1,5], **Jeremy S. Duffield**[1,3], **Mark W. Majesky**[1,4,5], and **Morayma Reyes**[1,2,6]

[1]Department of Pathology, School of Medicine, University of Washington

[2]Department of Oral Biology, School of Medicine, University of Washington

[3]Department of Medicine, School of Medicine, University of Washington

[4]Department of Pediatrics, Seattle Children's Research Institute

[5]Center for Cardiovascular Biology and Institute for Stem Cell and Regenerative Medicine, University of Washington

[6]Department of Laboratory Medicine, School of Medicine, University of Washington

Abstract

In Duchenne Muscular Dystrophy (DMD), progressive accumulation of cardiac fibrosis promotes heart failure. While the cellular origins of fibrosis in DMD hearts remain enigmatic, fibrotic tissue conspicuously forms near the coronary adventitia. Therefore, we sought to characterize the role of coronary adventitial cells in the formation of perivascular fibrosis. Utilizing the *mdx* model of DMD, we have identified a population of Sca1+, PDGFRα+, CD31−, CD45− coronary adventitial cells responsible for perivascular fibrosis. Histopathology of dystrophic hearts revealed Sca1+ cells extend from the adventitia and occupy regions of perivascular fibrosis. The number of Sca1+ adventitial cells increased two-fold in fibrotic *mdx* hearts vs. age matched wild-type hearts. Moreover, relative to Sca1−, PDGFRα+, CD31−, CD45− cells and endothelial cells, Sca1+ adventitial cells FACS-sorted from *mdx* hearts expressed the highest level of *Collagen1α1* and *3α1*, *Connective tissue growth factor*, and *Tgfβr1* transcripts. Surprisingly, *mdx* endothelial cells expressed the greatest level of the *Tgfβ1* ligand. Utilizing *Collagen1α1-GFP* reporter mice, we confirmed that the majority of Sca1+ adventitial cells expressed type I collagen, an abundant component of cardiac fibrosis, in both wt (71% ±4.1) and *mdx* (77% ±3.5) hearts. In contrast, GFP + interstitial fibroblasts were PDGFRα+ but negative for Sca1. Treatment of cultured *Collagen1α1-GFP+* adventitial cells with TGFβ1 resulted in increased collagen synthesis, whereas pharmacological inhibition of TGFβR1 signaling reduced the fibrotic response. Therefore, perivascular cardiac fibrosis by coronary adventitial cells may be mediated by TGFβ1 signaling. Our results implicate coronary endothelial cells in mediating cardiac fibrosis via transmural TGFβ signaling, and suggest that the coronary adventitia is a promising target for developing novel anti-fibrotic therapies.

Disclosure Statement

The authors concede no conflicts of interest in the publication of this manuscript.

Keywords

Muscular Dystrophy; fibrosis; TGFβ1; Sca1; type I collagen; perivascular; adventitia

1. Introduction

Duchenne Muscular Dystrophy (DMD) is a genetic X-linked disease characterized by the absence of the dystrophin protein and progressive muscle wasting [1, 2]. The majority of DMD patients develop cardiomyopathy and with the advent of ventilators, heart failure is emerging as the leading cause of mortality [3–5]. Cardiomyopathy in DMD is characterized by the accumulation of fibrosis which promotes heart dysfunction [6–8]. Perivascular fibrosis, described in many cardiac diseases processes including DMD, has been implicated in heart failure [9, 10]. Yet the cellular processes and molecular mechanisms that govern perivascular fibrosis in chronic diseases are poorly characterized [11]. By histopathology, the proximity of perivascular fibrosis to the coronary adventitia is difficult to overlook. Therefore, we set out to define the role of coronary adventitial cells in perivascular fibrosis. Utilizing the *mdx* mouse model of DMD [12], herein this report we have characterized a population of Sca1+, PDGFRα+, CD31−, CD45− cells that reside in the coronary adventitia, and produce collagen in proximity to perivascular fibrosis. Specifically, in *mdx* hearts we detected Sca1+ cells in regions of severe perivascular fibrosis. In turn, molecular analysis revealed that Sca1+ adventitial cells expressed significant levels of pro-fibrotic genes: *Collagen1α1*, *Collagen3α1*, *Tgfβr1*, and *Connective tissue growth factor (Ctgf)* [13–15]. Surprisingly, we observed that *mdx* endothelial cells expressed high levels of *Tgfβ1* ligand suggesting that adventitial cells become fibrotic via transmural TGFβ1 signaling. Indeed, stimulation of FACS-sorted adventitial cells with TGFβ1 *in vitro*, resulted in increased collagen expression and deposition. In contrast, pharmacological inhibition of TGFβR1 with SB525334 [16], resulted a reduction of collagen synthesis. Altogether, our findings indicate adventitial cells are associated with perivascular fibrosis and TGFβ1 signaling induces a fibrotic response in these cells.

2. Materials and Methods

2.1. Animals

All animal experiments were done in accordance with Institutional Animal Case and Use Committee (IACUC) approved procedures. *mdx* animals harboring the *Col1α1-GFP* reporter allele were generated in house by mating a wt male heterozygous for *Col1α1-GFP* allele, with *mdx* females. Since dystrophin is x-linked, the resulting male progeny were all *mdx* with a Mendelian inheritance frequency of ½ for the *Col1α1-GFP* allele. All mice reported in this manuscript are under a C57BL/6 background (Supplement Table. S1).

2.2. Histology and Staining

For WGA labeling depicted in Fig. 1A, 11 month old *Sca1-GFP* males (n=3) were first anesthetized with 100μl per 10mg mouse weight, of 2.5% (w/v) avertin (Sigma-Aldrich, St.Louis, MO) in PBS. Following anesthesia, animals were injected intravenously with 100μl of 1mg/ml WGA-Rhodamine (Vector Labs, Burlingame, CA) in PBS and euthanized 5 minutes following injection. Post euthanasia, animals were perfused in the left ventricle, first with PBS followed by 4% formaldehyde. Hearts were then excised and incubated in 4% formaldehyde for 2 hours at room temperature. Following fixation, hearts were incubated in PBS with sucrose beginning with 10% (w/v) and 20%, each for 30 minutes at 4°C, then transferred to 30% sucrose and left overnight at 4°C. The following day *Sca1-GFP* hearts were frozen in OCT in isopentane cooled by liquid nitrogen to negative 150–160°C. Tissue from *PDGFRα-GFP* and *:Co1a1-GFP* reporteranimals were fixed and processed in the same

manner as *Sca1-GFP* hearts, but without perfusion. Hearts from non-GFP reporter *mdx* animals used for cardiac histology were all males ranging from 12–22 months of age. These hearts were freshly frozen without prior fixation or processing. For picrosirius staining, tissue was fixed with ice cold methanol for 5 minutes, then stained in saturated picric acid containing 0.1% (w/v) sirius red and 0.1% (w/v) fast green, for 1 hour at room temperature. Slides were then washed in acidified water, dehydrated with ethanol gradient of 70–100%, and cleared with four washes of xylene. Subsequent slides from the same hearts were used to correlate picrosirius red staining with antibody staining. For antibody staining tissue was fixed with 4% formaldehyde for 5 minutes, washed with PBS, and blocked with PBS containing 10% goat or horse serum if the secondary antibody was goat, and 1% BSA for 20 minutes, at room temperature. All antibodies were diluted in PBS with 1% BSA. Control staining was run in parallel using an IgG isotype antibody made in rat, goat or rabbit, and subsequent secondary antibodies. Antibody specifics and dilutions are listed in supplement table S2. Epifluorescent photographs were taken with an Axiocam mRM monochrome camera using a Zeiss Axiovert 200 microscope with previously described components [17]. Confocal photographs (Fig. 4) were taken with a Nikon A1R system located in the Lynn and Mike Garvey cell imaging lab, at the University of Washington's Institute for Stem Cell and Regenerative Medicine (ISCRM imaging core). Channels were subsequently colored and merged using Adobe Photoshop CS2. To reduce background, brightness and contrast levels were adjusted when necessary. Brightness and contrast levels for controls were also adjusted in parallel under the same parameters.

2.3. Flow Cytometry

FACS was conducted as previously described but adjusted for smaller volumes to accommodate digesting whole hearts [17, 18]. For this hearts were excised, cleaned of any visible clots, washed in PBS and minced into ≤3mm pieces. Minced individual hearts were then digested in 3ml PBS containing a final concentration of 2 mM $CaCl_2$, 1.2units/ml Dispase II and 2 mg/ml Collagenase type IV (both from Worthington, Lakewood, NJ), for 45 minutes at 37°C. Every 15 minutes of the digestion, the tissue was triturated with a 1000μl pipette. Following 45 minutes of incubation, 4ml of HAM'S/F10 supplemented with 15% horse serum (Thermo/HyClone, Logan, UT) was added to each sample to inhibit the digestion. Samples were then passed through a 40μm cell strainer and then centrifuged at 300g rcf for 5 minutes. Following centrifugation, cells were resuspended in hemolysis buffer: 155 mM NH_4Cl, 10 mM $KHCO_3$ and 0.1 mM EDTA in H_2O. Following 5 minutes of hemolysis at room temperature, cells were centrifuged (300g rcf for 5 min) and washed in PBS+0.3% BSA to remove hemolysis buffer. Cells were centrifuged again to remover residual hemolytic buffer, and once more resuspended in PBS+0.3%, at 100μl per 10^6 cells. Prior to the addition of antibodies, cells were incubated with 1μg per 10^6 cells Fc receptor blocking antibody (purified anti-CD16/32) for 10 minutes on ice. We then added any biotin conjugated antibodies for 1 hour on ice, washed, and resuspended in PBS+0.3% containing a cocktail of antibodies and streptavidin that were directly conjugated to fluorophores. Cells were once more incubated on ice for 1 hour, washed and resuspended in PBS+0.3% at 500μl per 10^6 cells for analysis and sorting. We conducted all FACS acquisition and sorting with an Aria II (BD, San Jose, CA) with Diva software. Unstained and single color controls were used for compensation, which was automatically calculated by the Diva software. For analysis of GFP+ cells, hearts from GFP negative littermate were processed in parallel and used for the compensation controls. For RNA isolation, cells were directly sorted into 1.5ml eppendorf tubes containing 350μl RLT buffer (Qiagen, Valencia, CA), and placed on dry ice immediately following each sort. Antibody specifics (Supplement Table. S2–3) and combinations used (Supplement Table. S4) are listed below.

2.4. Cytocentrifuged Cells

Cells from *RGS5*$^{lacZ/+}$ reporter mice were FACS-sorted into DMEM with 10%FCS and immediately cytocentrifuged onto slides (Fisherbrand Super Frost Plus slides) at 800g rcf for 5 minutes. Slides were then fixed with 2% formaldehyde with 0.2% glutaraldehyde for 10 minutes, washed with PBS three times, and incubated with X-gal at 37°C overnight [19]. Following removal of the X-gal staining buffer, slides were washed and stained with eosin Y for 30 seconds, washed with water, and then dried for mounting.

2.5. Bone Marrow Chimeras

Generation of bone marrow chimeras was done as previously described [17]. Briefly, recipients were irradiated with two doses of 0.6Gy, 4 hours apart. Following the second dose of irradiation, we waited an additional 4 hours and then injected donor bone marrow cells via tail vein. Donor bone marrow cells were isolated from femurs of 4 month old female heterozygous for the chicken β-actin promoter driven EGFP allele [20]. Recipients were C57BL/6J males, 12.5 months old at the time of irradiation transplant. Recipients were euthanized and analyzed for bone marrow contribution 11 weeks post-transplant. Femur and tibia bone marrow cells were also analyzed for GFP to verify a sufficient degree of chimerism. Bone marrow chimerism of donor GFP cells was ≥90% relative to controls; bone marrow cells from a C57BL/6J mouse and from a chicken β-actin promoter driven EGFP mouse, both isolated and analyzed as negative and positive control in parallel to chimeras.

2.6. Quantitative-Reverse Transcription PCR

Freshly FACS-sorted cells were extracted for total RNA by using the RNeasy Mini Kit (Qiagen) according to the manufacturer's protocol. RNA quantity and purity was determined by 260/280 nm absorbance. First-strand cDNA was synthesized by using the High Capacity cDNA synthesis kit with a randomized primer (Applied Biosystems, Foster City, CA) following the manufacturer's protocol. qRT-PCR reactions using cDNA (20ng) were done as previously described using an ABI 7900HT PCR system, SYBRGreen/Rox PCR master mix (Fermentas, Glen Burnie, MD) for all reactions, and S.D.S software for analysis of comparative Ct method by the formula; $2^{-\Delta Ct}$, where $^{\Delta}Ct = Ct_{\text{target}} - Ct_{\textit{18S}\text{ rRNA}}$ [19]. For Fig. 3 we utilized $2^{-\Delta\Delta Ct} = Ct_{\text{target}} - Ct_{\textit{18S}\text{ rRNA sorted cells}} - Ct_{\textit{18S}\text{ rRNA unsorted cell,}}$ to compare samples within each group but not across groups (wt and *mdx*). All sample reactions were run in triplicate and normalized to *18S* rRNA. Ct values derived from each cell type and sample (e.g. each wt and *mdx* cell population was normalized to its own respective value for *18S*) or to *18S* of whole wt or *mdx* hearts respectively (Supplementary Fig. 7–8) to compare samples between wt and *mdx* groups. Error bars represent the standard error of mean calculated from three independent experiments. Primer sequences for *Ctgf*, *Tgfβ1*, *Mmp-2*, *Mmp-9* and *18S* were previously reported by Au.CG. et al (2011) [13]. Primers for *Collagen1α1*, *Collagen3α1* and *β-actin* were previously reported by Kenyon NJ. et al. (2003) [21]. *Tgfβr1* primers were reported by Zhou L. et al (2006) [22]. Primers for *Sca1* were developed by Primer Bank [23] [24, 25], while primers for *αSMA* and *SM22α* have been previously reported by Grabski A. et al (2009)[26]. Primers for *Collagen1α2* were reported by Onofre-Oliveira PC. et al (2012)[27]. *GAPDH* was previously reported by Ieronimakis N. et al (2008)[18]. Specific primer sequences are listed in supplement table S5. Average Ct values generated and used for analysis of Supplementary Fig. 7–8, for comparison of wt and *mdx* FACS-sorted populations are listed in the supplement table S6.

2.7. Statistical Analysis

P values were derived by two-tailed Student's *t*-test. Errors bars represent the standard error of the mean (SEM). Graphs and statistical calculations were generated using Microsoft Excel.

2.8 *In vitro* Culture and Experiments

Utilizing the aforementioned methods, GFP+ and GFP−, Sca1+, CD31−, CD45− cells were FACS-sorted from 4 month old *wt:Col1α1-GFP* hearts (n=3 GFP+ mice) and cultured in DMEM-HG with 10% FCS at 37°C, 5%CO_2 and 5%O_2. Both GFP+ and GFP− cells were maintained in culture and examined for the presence of GFP for 30 days. At this time GFP+ cells were pooled and expanded into two twelve well plates and grown to confluency for treatment with TGFβ1. For fibrogenic induction, 4 wells from each plate were treated with one of the following with DMEM-HG + 5% FCS as the basal media; 1) DMSO vehicle control, 2) TGFβ1 at a final concentration of 10ng/ml, 3) 10ng/ml TGFβ1 with 1μM of the TGFβR1 inhibitor (SB525334) [16]. Following 4 days of treatment, cells for collagen staining were fixed with 4% formaldehyde for 30 minutes then stained with picrosirius red for 1hour. Quantification of collagen by picrosirius red staining was done as percentage of area stained within individual fields as depicted in Fig. 6B, and normalized to the area measured using ImageJ v1.40. Cells collected for gene expression analysis were scraped and suspended in RLT lysis buffer (350μl per well of a 12 well plate) for RNA isolation, cDNA synthesis, and PCR analysis using the same reagents and methods/conditions outlined in section 2.6. Cells from *wt:PDGFRα-GFP* and *wt:Sca1-GFP* mice depicted in Supplemental Fig. 20–21, were also sorted and cultured under the same aforementioned conditions.

3. Results

3.1. Coronary adventitial cells extend to occupy perivascular fibrosis and are distinct from pericytes and inflammatory cells

Sca1 is a surface receptor associated with many cell types including macrovascular adventitial cells [28–30]. We initially examined wild-type (wt) hearts and observed that in addition to endothelial cells, coronary adventitial cells were also Sca1+. Utilizing the *Sca1-GFP* transgenic reporter mouse, we confirmed expression and co-localization of Sca1 to the coronary adventitia [31]. To distinguish the vascular endothelium which also expresses Sca1 in this model [18, 32–35], we intravenously (IV) injected the lectin wheat germ agglutinin (WGA) prior to euthanasia to label the vasculature. Histological survey of cross-sections from these hearts revealed *Sca1-GFP* + cells negative for IV injected-WGA, localized to the coronary adventitia (Fig. 1A) and distinguishable from endothelial cells (*Sca1-GFP*+ and positive for IV injected-WGA) and pericytes (NG2+, *Sca1-GFP* −) (Fig. 1B). Further characterization of Sca1+ coronary adventitial cells was performed in sections from *mdx* hearts by co-localization with picrosirius red, a dye that stains collagen and is routinely used for identifying fibrosis [36]. Sca1+ cells in *mdx* hearts were abundant within the coronary adventitia and distinguishable from BS1+ endothelial cells which also express Sca1 (Fig. 1C) [37]. Consistently, we observed Sca1+ cells extending from the coronary adventitia to proximal regions of severe perivascular fibrosis (Fig. 2 and Supplement Fig. 1). In older *mdx* hearts, Sca1+ cells occupied sizable regions of fibrosis throughout the myocardium (Supplement Fig. 2). This population of Sca1+ adventitial cells surrounding coronary arteries was also negative for CD31, expressed by endothelial and inflammatory cells, and CD45, a marker of hematopoietic cells (Supplement Fig. 3) [38, 39]. In concordance with our previously published work, we observed Sca1+, CD45+ inflammatory cells which were present in damaged regions of *mdx* hearts (Supplement Fig. 3C)[17]. However, analysis of bone marrow chimeras indicated that Sca1+ adventitial cells are not bone marrow-derived (Supplement Fig. 4). Moreover, we observed these cells were negative for Thy1, a receptor associated with cardiac fibroblasts, and $Rgs5^{lacZ}$, a reporter expressed by pericytes and smooth muscle cells (Supplement Fig. 5) [40, 41].

3.2. Molecular analysis reveals coronary adventitial cells express pro-fibrotic genes

To further characterize the Sca1+ coronary adventitial cells, we FACS-sorted the same population identified as Sca1+, CD31−, CD45− by histology, for gene expression analysis (Fig. 3A). For FACS-analysis and sorting, whole hearts were digested with collagenase and neutral protease, enzymes commonly used to produce single cell suspensions and retain cell surface antigens [19, 42–44]. FACS-analysis revealed that the majority of Sca1+, CD31−, CD45− cells are positive for PDGFRα and CD34 (Fig. 3B). PDGFRα signaling has been implicated in the formation of fibrosis and is expressed by fibrotic cells of the skeletal muscle [45], [46]. Conversely, CD34 is expressed by many cell types, including progenitor cells of the macrovascular adventitia [29]. In contrast, the Sca1+, CD31−, CD45− population was negative for CD133, a marker of circulating progenitors, and expressed only low levels of the fibroblast marker Thy1.2 (the C57BL/6 strain allele for Thy1) [47]. To compare the abundance Sca1+, CD31−, CD45− cells between wt and *mdx*, we calculated the number of cells per mg tissue by multiplying the proportion generated by FACS to number of cells counted following digestion over the initial weight of each heart [48]. In turn, the number of Sca1+, CD31−, CD45− cells was two-fold greater in *mdx* vs. wt hearts (Fig. 3C). Furthermore, the proportion of Sca1+ cells among the PDGFRα +, CD31−, CD45− population significantly increased in *mdx* hearts (Fig. 3C).

To survey the expression of genes implicated in fibrotic tissue formation, we FACS-sorted the Sca1+, CD31−, CD45− adventitial population directly into lysis/RNA isolation buffer for quantitative reverse-transcription PCR (qRT-PCR) analysis. In parallel we also sorted endothelial cells (Sca1+, CD31+, CD45−), interstitial fibroblasts (Sca1−, PDFGRα+, CD31−, CD45−) and macrophages (F4/80+, CD45+) which have been reported to mediate fibrosis via the TGFβ pathway [18, 45, 46, 49, 50]. For this comparison, we could only sort sufficient numbers of macrophages from *mdx* but not wt hearts. Results indicate that adventitial cells (Sca1+, CD31−, CD45− cells) and Sca1−, PDFGRα+, CD31−, CD45− cells express similar levels of *Collagen1α1* and *Collagen3α1* (Fig. 3D left graph) and *Ctgf*, *Tgfrβr1*, and *Tgfβ1* mRNA in wt hearts (Fig. 3E left graph). In contrast, Sca1+ adventitial cells isolated from *mdx* hearts expressed significantly greater levels of all these genes as compared to Sca1−, PDFGRα+, CD31−, CD45− cells isolated from the same *mdx* hearts (Fig. 3D right graph and 3E right graph). As previously reported for *mdx* whole heart tissue, the expression of *Collagen3α1* was also greater than C*ollagen1α1* in *mdx* cells [13]. Of note, type III collagen is a fibrillar collagen essential for vessel stability and is produced at greater levels than type I collagen by pro-fibrotic aortic adventitial cells [51, 52]. We also observed elevated expression of these pro-collagens in the right vs. left ventricles of 12 month old *mdx* mice (Supplementary Fig. 6), which have been shown to develop right ventricle dysfunction prior to left ventricle dysfunction [53, 54]. Surprisingly, relative to the other populations analyzed from *mdx* hearts, endothelial cells expressed the greatest level of the *Tgfβ1* ligand (Fig. 3E right graph). The expression of the majority of pro-fibrotic genes depicted in Fig. 3, was greater in *mdx* sorted cells for each respective population. A more comprehensive analysis indicates that the expression of these genes, with the exception of endothelial cell *Ctgf* expression, is elevated in *mdx* vs. wt sorted cells (supplement Fig. 7–8).

Immunostaining for the TGFβ1 ligand confirmed co-localization with microvascular endothelial cells around damaged regions of *mdx* hearts (Supplemental Fig. 9). Staining for TGFβ1 ligand was also observed in Sca1+ endothelial and adventitial cells of *mdx* coronary arteries (Supplemental Fig. 10). Staining for TGFβR1 was more diffuse and localized with most of the vasculature including adventitial and vascular smooth muscle cells. In contrast, TGFβR2 which mediates TGFβ signaling via phosphorylation of TGFβR1, co-localized with Sca1+ adventitial cells and endothelial cells lining the coronary arteries (Supplementary Fig. 11–12), [55, 56]. In addition to TGFβ1, endothelial cells expressed high levels of *Mmp-9,*

while Sca1+ adventitial cells expressed the greatest level of *Mmp-2* (Supplement Fig. 13); both of these MMPs covert latent TGFβ ligands to active forms [57]. Altogether, this gene expression profile and presence of TGFβ1 ligand and TGFβ receptors in the adventitia of *mdx* coronary arteries, indicates that Sca1+ adventitial cells respond to TGFβ1 and are pro-fibrotic in *mdx* hearts. These findings implicate the endothelium in promoting fibrosis via the TGFβ1 signaling pathway in response to chronic disease present in *mdx* hearts.

3.3. The majority of coronary adventitial cells express *Collagen1α1* and are distinguishable from interstitial fibroblasts by their expression of Sca1

Although these results suggest that Sca1+ adventitial cells contribute to perivascular fibrosis, the heterogeneity of fibrotic cells within this population remained unclear. Therefore, we utilized the *Collagen1α1-GFP* (*Col1α1-GFP*) reporter mice to analyze the proportion of fibrotic cells within this population [58]. Type I collagen is abundant in cardiac fibrosis and thus GFP expression in this model is indicative of fibrotic cells [58, 59]. For this we generated *mdx:Col1α1-GFP* mice and compared them to age matched wt:*Col1α1-GFP* animals (n=3 wt, n=3 *mdx*; 4 months old, all males) (Fig. 4 and Supplement Fig. 14). By FACS-analysis, the majority of Sca1+, CD31−, CD45− adventitial cells were GFP+ in both of wt (71% ±4.1) and *mdx* (77% ±3.5) hearts (Fig. 4A and Supplement Fig. 14A). In agreement with our qRT-PCR results (Fig. 3D), we detected GFP+ cells within the PDGFRα+, Sca1−, CD31−, CD45− population; 69% ±4.8 in wt and 47% ±12.9 in *mdx*, were GFP+ within this population (P=0.19 between wt vs. *mdx*). In contrast, we did not detect GFP+ cells within the hematopoietic (CD45+) or endothelial (CD31+, Sca1+, CD45−) cell populations from either wt or *mdx* hearts. Histological analysis of *mdx:Col1α1-GFP* hearts confirmed the anatomical position of Sca1+, PDGFRα+, GFP+ cells to the coronary adventitia and the presence of Sca1−, PDGFRα+, GFP+ in the interstitium (Fig. 4B–D). Sca1+, *Col1α1-GFP+* cells also co-localized with staining for collagen1 and fibronectin, in the adventitial space of coronary vessels of *mdx* hearts (Supplementary Fig. 15). Both collagen type I and fibronectin are extracellular matrix proteins abundant in fibrotic tissue and are directly regulated by TGFβ1 signaling [60] [61]. By FACS analysis the majority of cells expressing *Col1α1-GFP* were positive for PDGFRα + in both wt (89% ±1.3) and *mdx* (97% ±0.9) hearts (Supplement Fig. 8B). Further characterization showed that cardiac Sca1+, *Col1α1-GFP*+ cells were negative, while a minority of Sca1+, *Col1α1-GFP*− cells were positive (<5%) for c-Kit (Supplementary Fig. 16A); a marker associated with cardiac progenitors [62]. In addition, we confirmed the lack of *Sca1* expression in Sca1−, PDGFRα+, *Col1α1-GFP*+ sorted cells by qRT-PCR (Supplementary Fig. 16B).

Pericytes that express *Collagen1α1-GFP* have been reported to be fibrotic in the kidney [58]. However, Sca1+ adventitial cells identified by their position surrounding coronary smooth muscle and absence of NG2 staining (Fig. 1B), fall outside the anatomical and phenotypic definition of pericytes (Fig. 1B). In turn, the *Col1α1-GFP*+, Sca1− cells observed in the interstitial space were also negative for NG2 (Fig. 5). Utilizing the *PDGFRα-GFP* reporter mouse, we confirmed that coronary adventitial and non-pericyte (NG2 negative) interstitial cells express *PDGFRα* (Supplementary Fig. 17). Interestingly, *PDGFRα* expressing cells were also abundant in the macrovascular adventitia (Supplementary Fig. 18), which has been previously reported to express Sca1 [30]. These data suggest that additional collagen1 producing cells, including interstitial fibroblasts, are PDGFRα+ and distinguishable from pericytes; however, these cells are also distinguishable from adventitial cells by the absence of Sca1 expression.

3.4. Coronary adventitial derived cells become fibrotic via TGFβ1 signaling *in vitro*

To characterize the molecular mechanism of fibrosis, we FACS-sorted and cultured for *in vitro* study, adventitial cells (Sca1+, CD31−, CD45−) that were GFP+ (majority) and GFP− (minority) from wt:*Col1α1-GFP* hearts (n=3). In culture Sca1+, CD31−, CD45− sorted as GFP+ maintained *Col1α1-GFP* transgene expression, whereas Sca1+, CD31−, CD45− sorted as GFP− never expressed GFP within the 4 week time frame surveyed (Fig. 6A). In contrast, Sca1−, PDGFRα+, CD31−, CD45− cells sorted as GFP+ maintained *Col1α1-GFP* expression (Supplementary Fig. 12). Interestingly both Sca1+/−, GFP+ sorted populations that maintained *Col1α1-GFP* expression, gave rise to cells in culture with a smooth muscle like phenotype; positive for αSMA but negative for Sca1 (Supplementary Fig. 19). The apparent loss of *Sca1* expression by Sca1+ sorted cells occurred early in culture, while Sca1−, PDGFRα+ sorted cells remained negative for *Sca1* expression during the same time-course examined for both populations (Supplementary Fig. 20A). Within this same period, *PDGFRα* expression was maintained by both populations (Supplementary Fig. 20B). Interestingly, the expression of αSMA also occurred early in culture, as cells derived from both Sca1+ and Sca1− sorted populations stained positive at 36 hours in culture, and showed pronounced αSMA staining by day 7 in culture (Supplementary Fig. 21).

Despite being able to observe cells derived from both Sca1+ and Sca1− sorted populations early in culture, only cells derived from the Sca1+, CD31−, CD45− sorted population, were able to expand sufficiently for *in vitro* study. Under the given culture conditions, we were not able to sufficiently expand cells derived from both Sca1+, *Col1α1-GFP−*, CD31−, CD45− or Sca1−, PDGFRα+, *Col1α1-GFP+,* CD31−, CD45− sorted populations, for *in vitro* comparison with Sca1+, *Col1α1-GFP+* derived cells. Therefore, we could only assess the response of cultured cells derived from Sca1+ *Col1α1-GFP+* sorted cells (which maintained *Col1-GFP* expression), to TGFβ1 in order to gain insight on the role of pro-fibrotic signaling in adventitial cell mediated fibrosis.

For this assay, cultured cells were treated in parallel with the vehicle, 10ng/ml TGFβ1, or 10ng/ml TGFβ1 with 1μM SB525334, a potent inhibitor of TGFβR1 kinase activity that has been shown to reduce collagen production both *in vitro* and *in vivo* [16, 63]. All three treatments were tested in quadruplicate, two times; once for morphological analysis of collagen production with picrosirius red staining (Fig. 6B), and secondly for molecular analysis of pro-fibrotic gene expression by qRT-PCR (Fig. 6C). Results from both visual and molecular analyses' indicate that TGFβ1 stimulates adventitial derived cells to become fibrotic. Expression levels for *Collagens1α1, 1α2, and 3α1* increased dramatically with the addition of TGFβ1. In contrast to freshly sorted cells which expressed elevated levels of *Collagen3α1* (Fig. 3D), cultured adventitial cells expressed greater levels of type I pro-collagens in response to TGFβ1. TGFβ1 is known to stimulate the expression of both type I pro-collagens via Smad3 [64] [65, 66]. In contrast, the regulation of *Collagen3α1* expression is less understood and may require additional factors present *in vivo* that synergistically promote the production collagen type III over type I. Interestingly, exposure to TGFβ1 also increased expression of *Tgfβ1* and *Tgfβr1,* suggesting that an autocrine response may sustain the fibrotic response of activated adventitial cells. In contrast, inhibition of TGFβR1 signaling by SB525334, reduced picrosirius red staining and resulted in even lower expression of *Collagen1α1, 1α2* and *3α1* vs. vehicle control treated cells. Consequently, SB525334 treated cells showed reduced expression of *Tgfβ1* and *Tgfβr1*, suggesting that pharmacological inhibition of TGFβR1 kinase activity results in a feedback response that may decrease the fibrotic response of adventitial cells to TGFβ1.

In addition to our survey of pro-fibrotic genes, we examined the expression of smooth muscle associated genes, as we observed cultured cells stained positive for αSMA+ (Supplementary Fig. 19 and 21) and it has been reported that cells derived from the

macrovascular adventitia can give rise to smooth muscle like cells *in vitro* [29, 30, 67]. qRT-PCR analysis of freshly sorted Sca1+, *Col1α1-GFP* +, CD31−, CD45− cells (Supplementary Fig. 22A), indicates that *in vivo* coronary adventitial cells express almost undetectable levels of *αSMA* and *SM22α*;genes expressed by developing and mature smooth muscle cells [68–70]. In contrast, cells derived from this Sca1+, *Col1α1-GFP*+, CD31−, CD45− sorted population in culture, express *αSMA* and low levels of *SM22α* (Supplementary Fig. 22B). Treatment with TGFβ1, which results in upregulation of *Collagen1α1, 1α2 and 3α1,* and increased collagen deposition (Fig. 6), also significantly reduced the expression of these smooth muscle associated genes (Supplementary Fig. 22B). Therefore, it is possible that coronary adventitial cells can give rise to smooth muscle-like cells that can convert to a fibroblast phenotype in response to pro-fibrotic stimuli. However, without rigorous lineage tracing studies, we take caution in suggesting that this process occurs *in vivo* and is not exclusive to cell culture.

4. Discussion

Fibrosis is a primary indicator of disease progression in DMD [71]. Late gadolinium enhancement can detect fibrosis in the heart of DMD patients and corresponds with decreased ejection fraction and unfavorable left ventricle remodeling [72]. Progressive fibrosis has also been shown to perturb the hemodynamics of *mdx* hearts even following dystrophin rescue by AAV mediated gene therapy [54, 73]. Therefore, elucidating the molecular mechanisms and cellular processes that govern fibrosis, is critical for preventing or reversing cardiac dysfunction in muscular dystrophy.

Herein this report, we implicate coronary adventitial cells as the cell population associated with perivascular fibrosis. We have characterized these cells using a host of markers in relation to the anatomical position of the coronary adventitia. Interestingly, adventitial cells and interstitial fibroblasts expressed similar markers, but were distinguishable by the expression of Sca1. Numerous studies have reported that cardiac progenitor and/or stem cells also express Sca1 [74−76]. In turn, we did observe a minority of Sca1+, CD31−, CD45− cells were positive for c-Kit and did no express *Col1α1-GFP in vivo* or *in vitro.* In contrast, Sca1+, *Col1α1-GFP+* adventitial cells gave rise to Sca1− cells that maintained *PDGFRα* expression and began expressing smooth muscle associated genes in culture. Therefore, it is possible that Sca1+ coronary adventitial cells or a subset of progenitor within this population is capable of giving rise to smooth muscle like cells and/or Sca1−, PDGFRα + interstitial fibroblasts. Indeed, Hu et al., showed that Sca1+ cells from the aortic adventitia can contribute to smooth muscle like cells in the atherosclerotic lesion of *ApoE* null mice [29]. Given the close proximity of coronary adventitial cells to coronary endothelium, it is also possible that pro-fibrotic adventitial cells emerge via endothelial-to-mesenchymal transition [77], as both cell types share expression of *Sca1* and *Tgfβ1*. However, the focus of this report was to gain insight into the natural role of adventitial cells in cardiac fibrosis. Furthermore, without proper lineage tracing (e.g. lack of commercially available, inducible *Sca1-Cre* models) the relationship between putative Sca1+ stem cells and pro-fibrotic adventitial cells will remain enigmatic but warrants future investigation.

In retrospect, adventitial cells from wt hearts express genes characteristic of cardiac extracellular matrix including the *Col1α1-GFP* reporter, but were distinct from NG2+ pericytes that did not express the *Col1α1-GFP* transgene in the heart. In *mdx* hearts, we not only observe adventitial cells occupying regions of perivascular fibrosis, but the expression of fibrosis-related genes is elevated in comparison to wt hearts. Specifically, elevated expression of *Tgfβr1* by *mdx* adventitial cells implicated TGFβ1 signaling pathway as a potential molecular mechanism of perivascular fibrosis. Indeed, *in vitro* treatment of adventitial cells with TGFβ1 resulted in elevated collagen production suggesting TGFβ1

signaling may be implicated in *mdx* perivascular fibrosis. Accordingly, inhibition of TGFβ signaling has been shown to reduce fibrosis and improve skeletal muscle and cardiac function of *mdx* mice [78–81]. Importantly, we observed elevated expression of the *Tgfβ1* ligand in *mdx* derived coronary endothelial cells. These data suggest that the endothelium may play a role in the signaling of perivascular fibrosis in chronic disease (proposed model; Fig. 6D). Response to sheer stress has been reported to upregulate *Tgfβ1* expression in endothelial cells [82]. Incidentally, shear stress-induced endothelial vasodilation is reduced in *mdx* arteries [83]. Therefore, alterations in shear stress response and/or pressure overload in the vessel wall may trigger cardiac perivascular fibrosis in DMD and other chronic diseases [84, 85].

In summary, our findings provide new insights into the cellular interactions and signaling pathways responsible for perivascular fibrosis and identify the coronary adventitia as a novel target for development of anti-fibrotic therapies.

Supplementary Material

Refer to Web version on PubMed Central for supplementary material.

Acknowledgments

We thank Dr. Renee LeBoeuf and Frank Dastvan for providing the Sca1 qPCR primers and carotid artery cDNA.

Sources of Funding

This work was supported by the American Heart Association award 11BGIA7140028 to M.R. The Seattle Children's Research Institute and NIH RO1 HL-093594 to M.W.M. NIH grants HL087513 and HL094374 to W.M.M. The UW Nathan Shock Center of Excellence in the Basic Biology of Aging Genetic Approaches to Aging Training grant T32 AG000057 and Pancretan Association of America Venizelion Scholarship to N.I. And the Anandamahidol Foundation Scholarship of Thailand to K.J.

References

1. Deconinck N, Dan B. Pathophysiology of duchenne muscular dystrophy: current hypotheses. Pediatric neurology. 2007; 36:1–7. [PubMed: 17162189]
2. Culligan KG, Mackey AJ, Finn DM, Maguire PB, Ohlendieck K. Role of dystrophin isoforms and associated proteins in muscular dystrophy (review). International journal of molecular medicine. 1998; 2:639–48. [PubMed: 9850730]
3. Sultan A, Fayaz M. Prevalence of cardiomyopathy in Duchenne and Becker's muscular dystrophy. J Ayub Med Coll Abbottabad. 2008; 20:7–13. [PubMed: 19385447]
4. Spurney CF. Cardiomyopathy of Duchenne muscular dystrophy: current understanding and future directions. Muscle & nerve. 2011; 44:8–19. [PubMed: 21674516]
5. Eagle M, Baudouin SV, Chandler C, Giddings DR, Bullock R, Bushby K. Survival in Duchenne muscular dystrophy: improvements in life expectancy since 1967 and the impact of home nocturnal ventilation. Neuromuscul Disord. 2002; 12:926–9. [PubMed: 12467747]
6. Frankel KA, Rosser RJ. The pathology of the heart in progressive muscular dystrophy: epimyocardial fibrosis. Human pathology. 1976; 7:375–86. [PubMed: 939536]
7. Moriuchi T, Kagawa N, Mukoyama M, Hizawa K. Autopsy analyses of the muscular dystrophies. The Tokushima journal of experimental medicine. 1993; 40:83–93. [PubMed: 8211986]
8. Naruse H, Miyagi J, Arii T, Ohyanagi M, Iwasaki T, Jinnai K. The relationship between clinical stage, prognosis and myocardial damage in patients with Duchenne-type muscular dystrophy: five-year follow-up study. Annals of nuclear medicine. 2004; 18:203–8. [PubMed: 15233281]
9. Weisenfeld S, Messinger WJ. Cardiac involvement in progressive muscular dystrophy. American heart journal. 1952; 43:170–87. [PubMed: 14894420]

10. Dai Z, Aoki T, Fukumoto Y, Shimokawa H. Coronary perivascular fibrosis is associated with impairment of coronary blood flow in patients with non-ischemic heart failure. Journal of cardiology. 2012
11. Zhou L, Lu H. Targeting fibrosis in Duchenne muscular dystrophy. Journal of neuropathology and experimental neurology. 2010; 69:771–6. [PubMed: 20613637]
12. Quinlan JG, Hahn HS, Wong BL, Lorenz JN, Wenisch AS, Levin LS. Evolution of the mdx mouse cardiomyopathy: physiological and morphological findings. Neuromuscul Disord. 2004; 14:491–6. [PubMed: 15336690]
13. Au CG, Butler TL, Sherwood MC, Egan JR, North KN, Winlaw DS. Increased connective tissue growth factor associated with cardiac fibrosis in the mdx mouse model of dystrophic cardiomyopathy. International journal of experimental pathology. 2010; 92:57–65. [PubMed: 21121985]
14. Sun G, Haginoya K, Wu Y, Chiba Y, Nakanishi T, Onuma A, et al. Connective tissue growth factor is overexpressed in muscles of human muscular dystrophy. Journal of the neurological sciences. 2008; 267:48–56. [PubMed: 17996907]
15. Lijnen PJ, Petrov VV, Fagard RH. Induction of cardiac fibrosis by transforming growth factor-beta(1). Molecular genetics and metabolism. 2000; 71:418–35. [PubMed: 11001836]
16. Grygielko ET, Martin WM, Tweed C, Thornton P, Harling J, Brooks DP, et al. Inhibition of gene markers of fibrosis with a novel inhibitor of transforming growth factor-beta type I receptor kinase in puromycin-induced nephritis. The Journal of pharmacology and experimental therapeutics. 2005; 313:943–51. [PubMed: 15769863]
17. Ieronimakis N, Hays A, Reyes M. Bone marrow-derived cells do not engraft into skeletal muscle microvasculature but promote angiogenesis after acute injury. Experimental hematology. 2012; 40:238–49. e3. [PubMed: 22155292]
18. Ieronimakis N, Balasundaram G, Reyes M. Direct isolation, culture and transplant of mouse skeletal muscle derived endothelial cells with angiogenic potential. PloS one. 2008; 3:e0001753. [PubMed: 18335025]
19. Ieronimakis N, Balasundaram G, Rainey S, Srirangam K, Yablonka-Reuveni Z, Reyes M. Absence of CD34 on murine skeletal muscle satellite cells marks a reversible state of activation during acute injury. PloS one. 2008; 5:e10920. [PubMed: 20532193]
20. Okabe M, Ikawa M, Kominami K, Nakanishi T, Nishimune Y. 'Green mice' as a source of ubiquitous green cells. FEBS letters. 1997; 407:313–9. [PubMed: 9175875]
21. Kenyon NJ, Ward RW, McGrew G, Last JA. TGF-beta1 causes airway fibrosis and increased collagen I and III mRNA in mice. Thorax. 2003; 58:772–7. [PubMed: 12947136]
22. Zhou L, Porter JD, Cheng G, Gong B, Hatala DA, Merriam AP, et al. Temporal and spatial mRNA expression patterns of TGF-beta1, 2, 3 and TbetaRI, II, III in skeletal muscles of mdx mice. Neuromuscul Disord. 2006; 16:32–8. [PubMed: 16373085]
23. Wang X, Seed B. A PCR primer bank for quantitative gene expression analysis. Nucleic acids research. 2003; 31:e154. [PubMed: 14654707]
24. Spandidos A, Wang X, Wang H, Dragnev S, Thurber T, Seed B. A comprehensive collection of experimentally validated primers for Polymerase Chain Reaction quantitation of murine transcript abundance. BMC genomics. 2008; 9:633. [PubMed: 19108745]
25. Spandidos A, Wang X, Wang H, Seed B. PrimerBank: a resource of human and mouse PCR primer pairs for gene expression detection and quantification. Nucleic acids research. 2010; 38:D792–9. [PubMed: 19906719]
26. Grabski AD, Shimizu T, Deou J, Mahoney WM Jr, Reidy MA, Daum G. Sphingosine-1-phosphate receptor-2 regulates expression of smooth muscle alpha-actin after arterial injury. Arteriosclerosis, thrombosis, and vascular biology. 2009; 29:1644–50.
27. Onofre-Oliveira PC, Santos AL, Martins PM, Ayub-Guerrieri D, Vainzof M. Differential expression of genes involved in the degeneration and regeneration pathways in mouse models for muscular dystrophies. Neuromolecular medicine. 2012; 14:74–83. [PubMed: 22362587]
28. Holmes C, Stanford WL. Concise review: stem cell antigen-1: expression, function, and enigma. Stem cells (Dayton, Ohio). 2007; 25:1339–47.

29. Hu Y, Zhang Z, Torsney E, Afzal AR, Davison F, Metzler B, et al. Abundant progenitor cells in the adventitia contribute to atherosclerosis of vein grafts in ApoE-deficient mice. The Journal of clinical investigation. 2004; 113:1258–65. [PubMed: 15124016]
30. Passman JN, Dong XR, Wu SP, Maguire CT, Hogan KA, Bautch VL, et al. A sonic hedgehog signaling domain in the arterial adventitia supports resident Sca1+ smooth muscle progenitor cells. Proceedings of the National Academy of Sciences of the United States of America. 2008; 105:9349–54. [PubMed: 18591670]
31. Ma X, Robin C, Ottersbach K, Dzierzak E. The Ly-6A (Sca-1) GFP transgene is expressed in all adult mouse hematopoietic stem cells. Stem cells (Dayton, Ohio). 2002; 20:514–21.
32. Kotton DN, Summer RS, Sun X, Ma BY, Fine A. Stem cell antigen-1 expression in the pulmonary vascular endothelium. American journal of physiology. 2003; 284:L990–6. [PubMed: 12611818]
33. Stuelsatz P, Keire P, Almuly R, Yablonka-Reuveni Z. A contemporary atlas of the mouse diaphragm: myogenicity, vascularity, and the Pax3 connection. The journal of histochemistry and cytochemistry: official journal of the Histochemistry Society. 2012; 60:638–57. [PubMed: 22723526]
34. Kirillova I, Gussoni E, Goldhamer DJ, Yablonka-Reuveni Z. Myogenic reprogramming of retina-derived cells following their spontaneous fusion with myotubes. Developmental biology. 2007; 311:449–63. [PubMed: 17919536]
35. Day K, Paterson B, Yablonka-Reuveni Z. A distinct profile of myogenic regulatory factor detection within Pax7+ cells at S phase supports a unique role of Myf5 during posthatch chicken myogenesis. Developmental dynamics: an official publication of the American Association of Anatomists. 2009; 238:1001–9. [PubMed: 19301399]
36. Whittaker P, Kloner RA, Boughner DR, Pickering JG. Quantitative assessment of myocardial collagen with picrosirius red staining and circularly polarized light. Basic research in cardiology. 1994; 89:397–410. [PubMed: 7535519]
37. Yeh HI, Dupont E, Coppen S, Rothery S, Severs NJ. Gap junction localization and connexin expression in cytochemically identified endothelial cells of arterial tissue. J Histochem Cytochem. 1997; 45:539–50. [PubMed: 9111232]
38. Scholz D, Schaper J. Platelet/endothelial cell adhesion molecule-1 (PECAM-1) is localized over the entire plasma membrane of endothelial cells. Cell and tissue research. 1997; 290:623–31. [PubMed: 9369538]
39. Stelzer GT, Shults KE, Loken MR. CD45 gating for routine flow cytometric analysis of human bone marrow specimens. Annals of the New York Academy of Sciences. 1993; 677:265–80. [PubMed: 8494214]
40. Hudon-David F, Bouzeghrane F, Couture P, Thibault G. Thy-1 expression by cardiac fibroblasts: lack of association with myofibroblast contractile markers. Journal of molecular and cellular cardiology. 2007; 42:991–1000. [PubMed: 17395197]
41. Nisancioglu MH, Mahoney WM Jr, Kimmel DD, Schwartz SM, Betsholtz C, Genove G. Generation and characterization of rgs5 mutant mice. Molecular and cellular biology. 2008; 28:2324–31. [PubMed: 18212066]
42. Kuang S, Kuroda K, Le Grand F, Rudnicki MA. Asymmetric self-renewal and commitment of satellite stem cells in muscle. Cell. 2007; 129:999–1010. [PubMed: 17540178]
43. Sacco A, Doyonnas R, Kraft P, Vitorovic S, Blau HM. Self-renewal and expansion of single transplanted muscle stem cells. Nature. 2008; 456:502–6. [PubMed: 18806774]
44. Jackaman C, Nowak KJ, Ravenscroft G, Lim EM, Clement S, Laing NG. Novel application of flow cytometry: determination of muscle fiber types and protein levels in whole murine skeletal muscles and heart. Cell motility and the cytoskeleton. 2007; 64:914–25. [PubMed: 17922482]
45. Uezumi A, Ito T, Morikawa D, Shimizu N, Yoneda T, Segawa M, et al. Fibrosis and adipogenesis originate from a common mesenchymal progenitor in skeletal muscle. Journal of cell science. 124:3654–64. [PubMed: 22045730]
46. Olson LE, Soriano P. Increased PDGFRalpha activation disrupts connective tissue development and drives systemic fibrosis. Developmental cell. 2009; 16:303–13. [PubMed: 19217431]

47. Timmermans F, Plum J, Yoder MC, Ingram DA, Vandekerckhove B, Case J. Endothelial progenitor cells: identity defined? Journal of cellular and molecular medicine. 2009; 13:87–102. [PubMed: 19067770]
48. Bonner F, Borg N, Burghoff S, Schrader J. Resident cardiac immune cells and expression of the ectonucleotidase enzymes CD39 and CD73 after ischemic injury. PloS one. 2012; 7:e34730. [PubMed: 22514659]
49. Austyn JM, Gordon S. F4/80, a monoclonal antibody directed specifically against the mouse macrophage. European journal of immunology. 1981; 11:805–15. [PubMed: 7308288]
50. Vidal B, Serrano AL, Tjwa M, Suelves M, Ardite E, De Mori R, et al. Fibrinogen drives dystrophic muscle fibrosis via a TGFbeta/alternative macrophage activation pathway. Genes & development. 2008; 22:1747–52. [PubMed: 18593877]
51. Liu X, Wu H, Byrne M, Krane S, Jaenisch R. Type III collagen is crucial for collagen I fibrillogenesis and for normal cardiovascular development. Proceedings of the National Academy of Sciences of the United States of America. 1997; 94:1852–6. [PubMed: 9050868]
52. Goel SA, Guo LW, Shi XD, Kundi R, Sovinski G, Seedial S, et al. Preferential secretion of collagen type 3 versus type 1 from adventitial fibroblasts stimulated by TGF-beta/Smad3-treated medial smooth muscle cells. Cellular signalling. 2013; 25:955–60. [PubMed: 23280188]
53. Zhang W, ten Hove M, Schneider JE, Stuckey DJ, Sebag-Montefiore L, Bia BL, et al. Abnormal cardiac morphology, function and energy metabolism in the dystrophic mdx mouse: an MRI and MRS study. Journal of molecular and cellular cardiology. 2008; 45:754–60. [PubMed: 18929569]
54. Stuckey DJ, Carr CA, Camelliti P, Tyler DJ, Davies KE, Clarke K. In vivo MRI characterization of progressive cardiac dysfunction in the mdx mouse model of muscular dystrophy. PloS one. 2012; 7:e28569. [PubMed: 22235247]
55. Wrana JL, Attisano L, Carcamo J, Zentella A, Doody J, Laiho M, et al. TGF beta signals through a heteromeric protein kinase receptor complex. Cell. 1992; 71:1003–14. [PubMed: 1333888]
56. Wrana JL, Attisano L, Wieser R, Ventura F, Massague J. Mechanism of activation of the TGF-beta receptor. Nature. 1994; 370:341–7. [PubMed: 8047140]
57. Bujak M, Frangogiannis NG. The role of TGF-beta signaling in myocardial infarction and cardiac remodeling. Cardiovascular research. 2007; 74:184–95. [PubMed: 17109837]
58. Lin SL, Kisseleva T, Brenner DA, Duffield JS. Pericytes and perivascular fibroblasts are the primary source of collagen-producing cells in obstructive fibrosis of the kidney. The American journal of pathology. 2008; 173:1617–27. [PubMed: 19008372]
59. Bishop JE, Greenbaum R, Gibson DG, Yacoub M, Laurent GJ. Enhanced deposition of predominantly type I collagen in myocardial disease. Journal of molecular and cellular cardiology. 1990; 22:1157–65. [PubMed: 2095438]
60. Villarreal FJ, Dillmann WH. Cardiac hypertrophy-induced changes in mRNA levels for TGF-beta 1, fibronectin, and collagen. The American journal of physiology. 1992; 262:H1861–6. [PubMed: 1535758]
61. Serini G, Bochaton-Piallat ML, Ropraz P, Geinoz A, Borsi L, Zardi L, et al. The fibronectin domain ED-A is crucial for myofibroblastic phenotype induction by transforming growth factor-beta1. The Journal of cell biology. 1998; 142:873–81. [PubMed: 9700173]
62. Beltrami AP, Barlucchi L, Torella D, Baker M, Limana F, Chimenti S, et al. Adult cardiac stem cells are multipotent and support myocardial regeneration. Cell. 2003; 114:763–76. [PubMed: 14505575]
63. Higashiyama H, Yoshimoto D, Kaise T, Matsubara S, Fujiwara M, Kikkawa H, et al. Inhibition of activin receptor-like kinase 5 attenuates bleomycin-induced pulmonary fibrosis. Experimental and molecular pathology. 2007; 83:39–46. [PubMed: 17274978]
64. Chen SJ, Yuan W, Lo S, Trojanowska M, Varga J. Interaction of smad3 with a proximal smad-binding element of the human alpha2(I) procollagen gene promoter required for transcriptional activation by TGF-beta. Journal of cellular physiology. 2000; 183:381–92. [PubMed: 10797313]
65. Ritzenthaler JD, Goldstein RH, Fine A, Lichtler A, Rowe DW, Smith BD. Transforming-growth-factor-beta activation elements in the distal promoter regions of the rat alpha 1 type I collagen gene. The Biochemical journal. 1991; 280 (Pt 1):157–62. [PubMed: 1741743]

66. Rossi P, Karsenty G, Roberts AB, Roche NS, Sporn MB, de Crombrugghe B. A nuclear factor 1 binding site mediates the transcriptional activation of a type I collagen promoter by transforming growth factor-beta. Cell. 1988; 52:405–14. [PubMed: 2830985]

67. Majesky MW, Dong XR, Hoglund V, Mahoney WM Jr, Daum G. The adventitia: a dynamic interface containing resident progenitor cells. Arteriosclerosis, thrombosis, and vascular biology. 2011; 31:1530–9.

68. Solway J, Seltzer J, Samaha FF, Kim S, Alger LE, Niu Q, et al. Structure and expression of a smooth muscle cell-specific gene, SM22 alpha. The Journal of biological chemistry. 1995; 270:13460–9. [PubMed: 7768949]

69. Lees-Miller JP, Heeley DH, Smillie LB, Kay CM. Isolation and characterization of an abundant and novel 22-kDa protein (SM22) from chicken gizzard smooth muscle. The Journal of biological chemistry. 1987; 262:2988–93. [PubMed: 3818630]

70. Li L, Miano JM, Cserjesi P, Olson EN. SM22 alpha, a marker of adult smooth muscle, is expressed in multiple myogenic lineages during embryogenesis. Circulation research. 1996; 78:188–95. [PubMed: 8575061]

71. Desguerre I, Mayer M, Leturcq F, Barbet JP, Gherardi RK, Christov C. Endomysial fibrosis in Duchenne muscular dystrophy: a marker of poor outcome associated with macrophage alternative activation. Journal of neuropathology and experimental neurology. 2009; 68:762–73. [PubMed: 19535995]

72. Puchalski MD, Williams RV, Askovich B, Sower CT, Hor KH, Su JT, et al. Late gadolinium enhancement: precursor to cardiomyopathy in Duchenne muscular dystrophy? The international journal of cardiovascular imaging. 2009; 25:57–63. [PubMed: 18686011]

73. Bostick B, Shin JH, Yue Y, Wasala NB, Lai Y, Duan D. AAV micro-dystrophin gene therapy alleviates stress-induced cardiac death but not myocardial fibrosis in >21-m-old mdx mice, an end-stage model of Duchenne muscular dystrophy cardiomyopathy. Journal of molecular and cellular cardiology. 2012; 53:217–22. [PubMed: 22587991]

74. Matsuura K, Nagai T, Nishigaki N, Oyama T, Nishi J, Wada H, et al. Adult cardiac Sca-1-positive cells differentiate into beating cardiomyocytes. The Journal of biological chemistry. 2004; 279:11384–91. [PubMed: 14702342]

75. Wang X, Hu Q, Nakamura Y, Lee J, Zhang G, From AH, et al. The role of the sca-1+/CD31− cardiac progenitor cell population in postinfarction left ventricular remodeling. Stem cells (Dayton, Ohio). 2006; 24:1779–88.

76. Oh H, Bradfute SB, Gallardo TD, Nakamura T, Gaussin V, Mishina Y, et al. Cardiac progenitor cells from adult myocardium: homing, differentiation, and fusion after infarction. Proceedings of the National Academy of Sciences of the United States of America. 2003; 100:12313–8. [PubMed: 14530411]

77. Zeisberg EM, Tarnavski O, Zeisberg M, Dorfman AL, McMullen JR, Gustafsson E, et al. Endothelial-to-mesenchymal transition contributes to cardiac fibrosis. Nature medicine. 2007; 13:952–61.

78. Huebner KD, Jassal DS, Halevy O, Pines M, Anderson JE. Functional resolution of fibrosis in mdx mouse dystrophic heart and skeletal muscle by halofuginone. American journal of physiology Heart and circulatory physiology. 2008; 294:H1550–61. [PubMed: 18263710]

79. Lorts A, Schwanekamp JA, Baudino TA, McNally EM, Molkentin JD. Deletion of periostin reduces muscular dystrophy and fibrosis in mice by modulating the transforming growth factor-beta pathway. Proceedings of the National Academy of Sciences of the United States of America. 2012; 109:10978–83. [PubMed: 22711826]

80. Nelson CA, Hunter RB, Quigley LA, Girgenrath S, Weber WD, McCullough JA, et al. Inhibiting TGF-beta activity improves respiratory function in mdx mice. The American journal of pathology. 2011; 178:2611–21. [PubMed: 21641384]

81. Van Erp C, Irwin NG, Hoey AJ. Long-term administration of pirfenidone improves cardiac function in mdx mice. Muscle & nerve. 2006; 34:327–34. [PubMed: 16770778]

82. Cucina A, Sterpetti AV, Borrelli V, Pagliei S, Cavallaro A, D'Angelo LS. Shear stress induces transforming growth factor-beta 1 release by arterial endothelial cells. Surgery. 1998; 123:212–7. [PubMed: 9481408]

83. Loufrani L, Matrougui K, Gorny D, Duriez M, Blanc I, Levy BI, et al. Flow (shear stress)-induced endothelium-dependent dilation is altered in mice lacking the gene encoding for dystrophin. Circulation. 2001; 103:864–70. [PubMed: 11171796]

84. Kamogawa Y, Biro S, Maeda M, Setoguchi M, Hirakawa T, Yoshida H, et al. Dystrophin-deficient myocardium is vulnerable to pressure overload in vivo. Cardiovascular research. 2001; 50:509–15. [PubMed: 11376626]

85. Wheeler MT, McNally EM. The interaction of coronary tone and cardiac fibrosis. Current atherosclerosis reports. 2005; 7:219–26. [PubMed: 15811257]

Highlights

- Adventitial cells extend appear to occupy perivascular fibrosis in *mdx* hearts.
- In *mdx* hearts Adventitial cells express elevated levels of pro-fibrotic genes.
- Endothelial cells derived from *mdx* hearts express elevated levels TGFβ1 ligand.
- The majority of adventitial cells express *Col1α1-GFP*, a reporter of fibrotic cells.
- Adventitial cells give rise to pro-fibrotic cells in response to TGFβ1 *in vitro*.

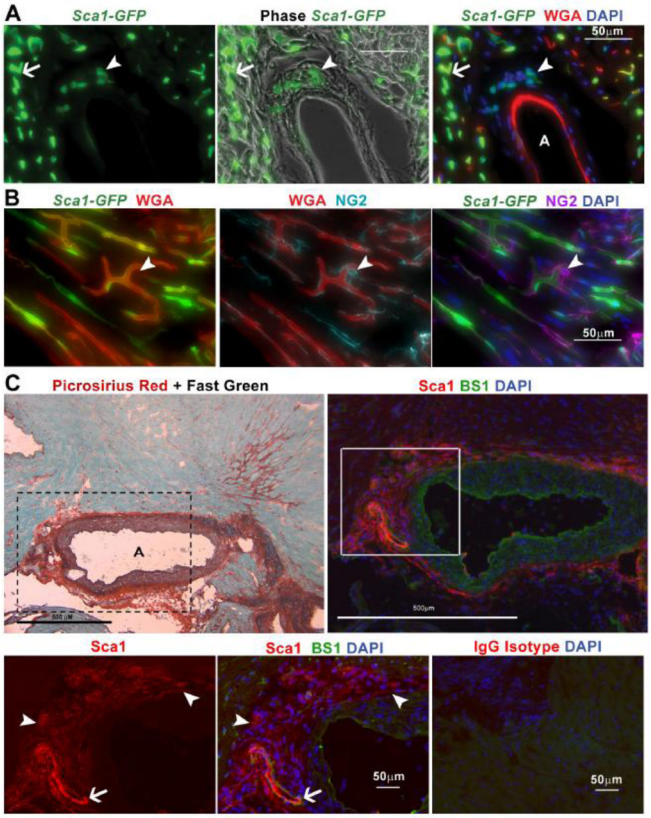

Fig. 1.

Sca1+ cells, distinct from endothelial cells and pericytes, reside in the coronary adventitia. A. Histological analysis of hearts from 11 month old *Sca1-GFP* animals injected intravenously with WGA, reveals coronary adventitial cells are *Sca1+* (arrowhead) and distinct from GFP+, IV injected-WGA+ endothelial cells (arrow) B. Staining for NG2 indicates pericytes (arrowhead) are negative for *Sca1-GFP* but cover GFP+, IV injected-WGA+ vascular endothelial cells. C. Staining with picrosirius red and fast green or Sca1 and BS1 in sections from a 22 month old *mdx* heart, reveals that collagen deposition surrounding the coronary adventitia is occupied by Sca1+, BS1− cells. A higher magnification (boxed area represented in bottom row) photo highlights adventitial Sca1+, BS1− cells (arrowhead) and Sca1+, BS1+ endothelial cells (arrow). The bottom right panel shows a serial section of the same *mdx* heart shown in C, stained in parallel with an IgG isotype antibody control. Coronary arteries are denoted with an A.

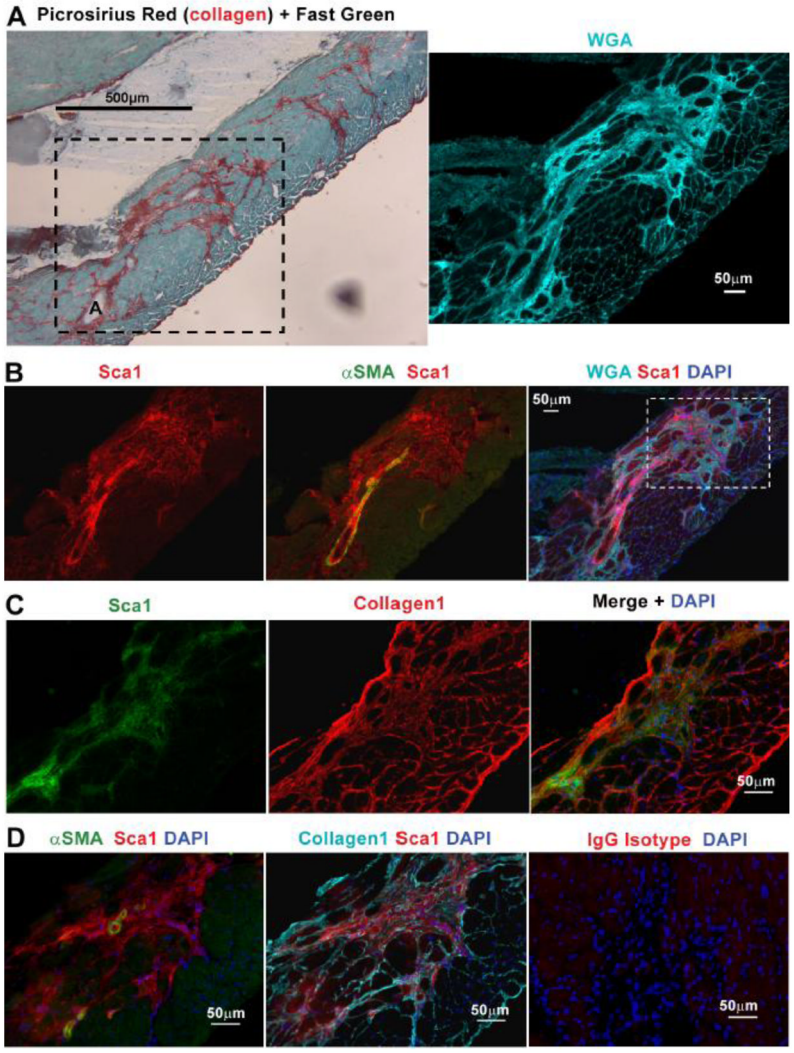

Fig. 2.

Sca1+ cells extend from the adventitia and occupy regions of perivascular fibrosis. A. Picrosirius red-fast green staining reveals perivascular fibrosis in 22 month old *mdx* hearts extending from coronary arteries. The boxed area depicts a serial section of the same region stained with WGA, which highlights the perivascular fibrosis depicted in by picrosirius red staining. The A denotes a coronary artery. B. Sca1+ cells are observed extending from the adventitia of α-smooth muscle actin+ (αSMA) coronary arteries, to occupy the corresponding fibrotic area that stained brightly positive with WGA (same staining shown in the right panel of A). C. Staining for type I collagen in serial sections from the same heart highlights the occupation of this fibrotic area (boxed region in the merge of B) by Sca1+ cells. D. A higher magnification photo of the same area shown in C, depicts Sca1 with αSMA and collagen1 staining's respectively. The far right panel depicts a section stained in parallel with an IgG isotype antibody to exclude the presence of non-specific staining.

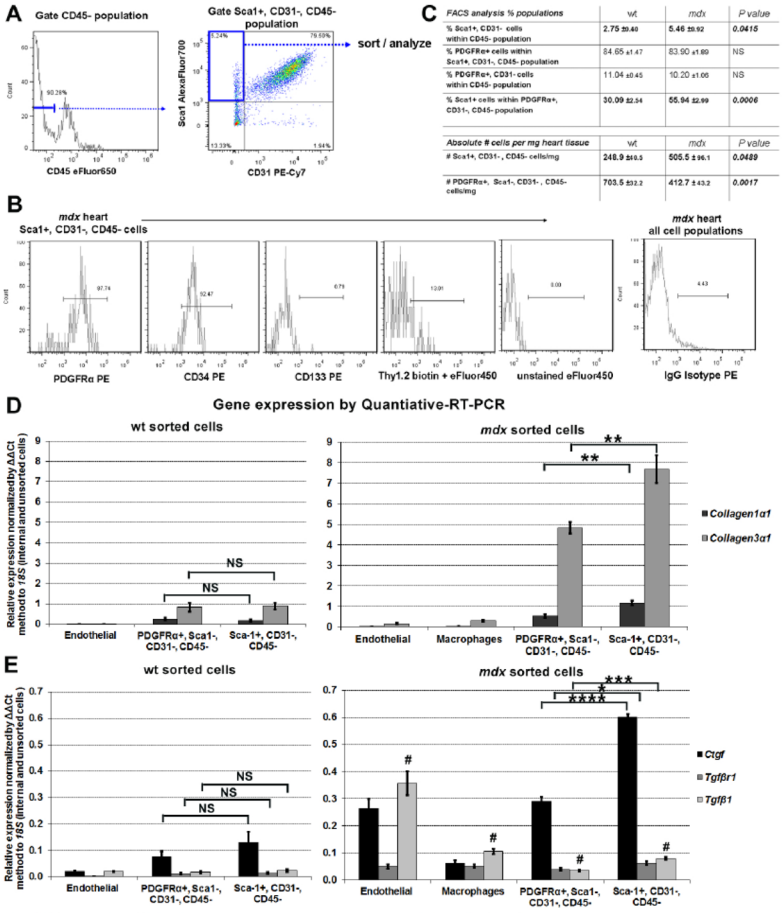

Fig. 3.

Sca1+ adventitial cells express markers and genes associated with fibrosis. A. Representative flow cytometry gating used for selecting the Sca1+, CD31−, CD45− adventitial population from cell suspensions isolated from wt and *mdx* hearts. B. analysis of *mdx* cells using a panel of antibodies shows the Sca1+, CD31−, CD45− population is predominantly PDGFRα + and CD34+, but CD133− and Thy1.2−. Unstained and IgG isoptype controls were used for gating analysis. C. Analysis of heart cells from 1 year old wt (n=4) vs. *mdx* (n=4) males, revealed that the proportion and absolute number of Sca1+ adventitial cells doubles in *mdx* hearts. In contrast, the number of PDGFRα+, Sca1−, CD31−, CD45− cells decline, indicating that Sca1+ cells become the predominant PDGFRα + cells in *mdx* hearts. D and E. Quantitative-RT-PCR analysis of freshly sorted cells (from1 year old males, n=4 wt and n=4 *mdx* hearts) reveals that in comparison to endothelial cells (Sca1+, CD31+, CD45-) and macrophages (CD45+, F4/80+), the PDGFRα+, Sca1−, CD31−, CD45− population and Sca1+, CD31−, CD45− adventitial cells both express genes indicative of fibrosis. Although not significantly (NS) different in wt, expression of these genes was significantly elevated in *mdx* adventitial cells. Surprisingly, endothelial cells from *mdx* hearts expressed the highest levels of the *Tgfβ1* ligand. Each sample was normalized to its respective expression of *18S*. * P<0.05, **P<0.005, ***P<0.0005. # denotes P<0.005 between endothelial cells vs. remaining populations. Error bars represent SEM, P values were derived from Student's *t*-test.

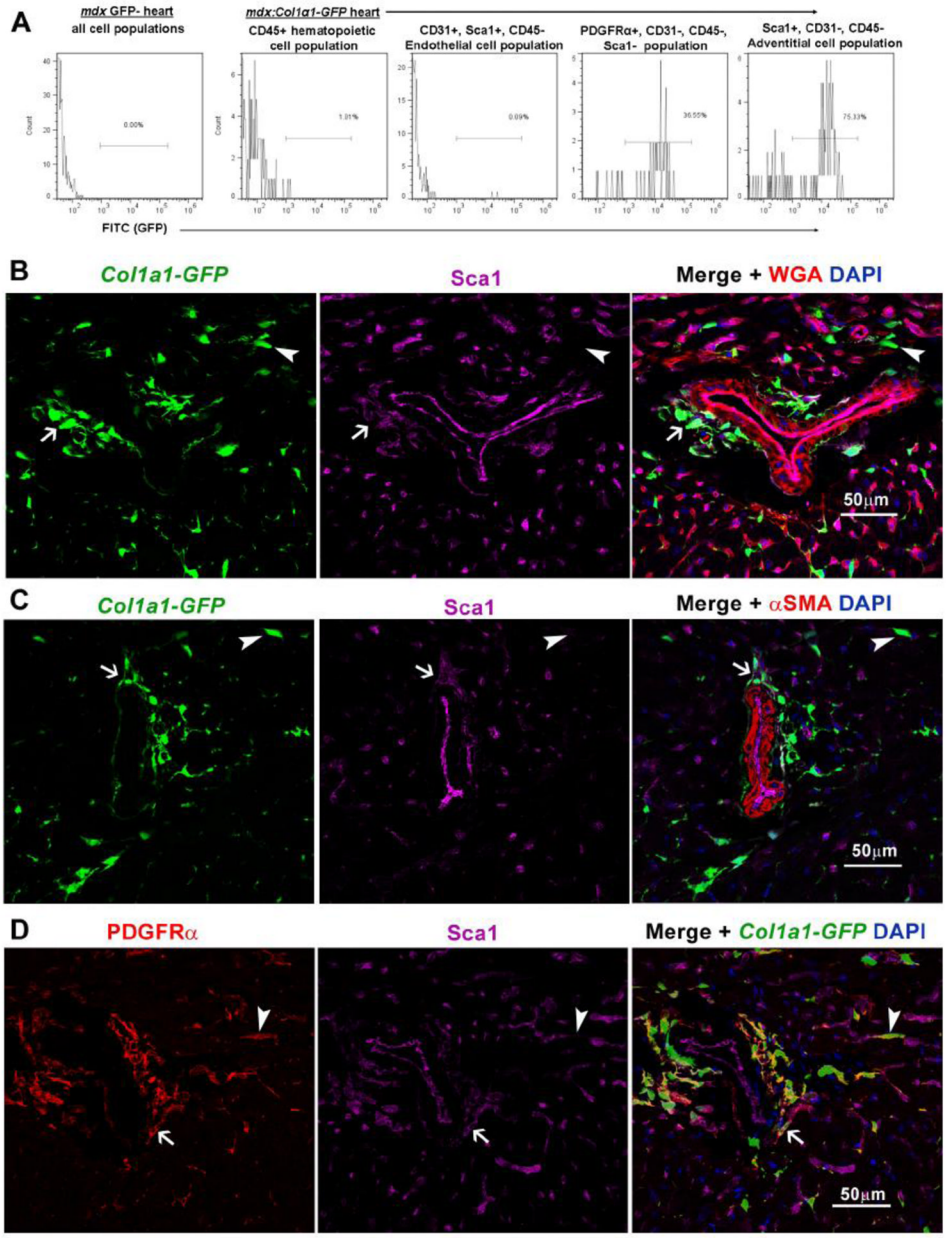

Fig. 4.

The majority of Sca1+ adventitial cells express *Collagen1α1-GFP* and are distinguishable from Sca1− interstitial fibroblasts. A. FACS-analysis of *mdx:Col1α1-GFP* hearts (n=3 GFP + and n=1 GFP− control, 4 month old males) reveals that the majority of Sca1+, CD31−, CD45− adventitial cells are GFP+. In turn, the highest proportion of GFP+ cells was observed in the Sca1+ adventitial cells vs. other populations analyzed. B. Histological analysis of an aged matched *mdx:Col1α1-GFP* heart, confirms the presence of Sca1+, GFP+ cells (arrow) in the adventitia of coronary arteries. In contrast, Sca1−, GFP+ interstitial cells (arrowhead) were visible near WGA+, Sca1+ endothelial cells. C. αSMA staining highlights the anatomical location of Sca1+, GFP+ (arrow) adventitial cells vs. Sca1−, GFP+ (arrowhead) interstitial fibroblasts. D. Staining for PDGFRα confirms the presence of

PDGFRα+, GFP+ interstitial fibroblasts (arrowhead), distinguishable from Sca1+ adventitial cells (arrow).

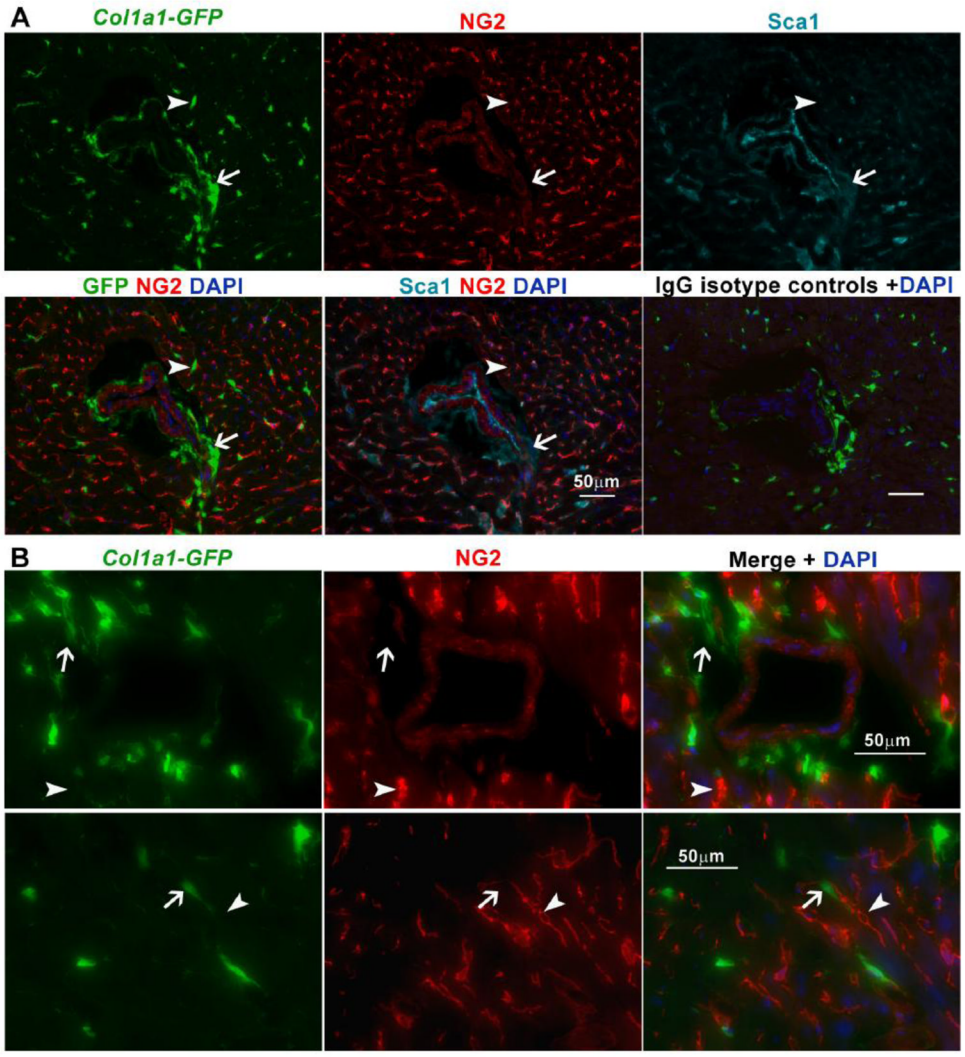

Fig. 5.

Collagen1α1-GFP+ cells are adventitial cells and fibroblasts distinct from pericytes. A. Staining for the pericyte marker NG2 indicates that GFP+ cells in *mdx:Col1α1-GFP* hearts are distinct from pericytes. As shown, Sca1+, GFP+ adventitial cells (arrow) and Sca1−, GFP+ interstitial cells (arrow) were both negative for NG2. The bottom right panel represent *mdx:Col1α1-GFP* heart tissue stained in parallel with IgG isotype controls for both Sca1 and NG2 antibodies. B. Higher magnification of a separate coronary vessel (top row) and interstitial space (bottom row), highlight the presence of NG2+, GFP− pericytes (arrowhead) vs. GFP+ cells (arrow).

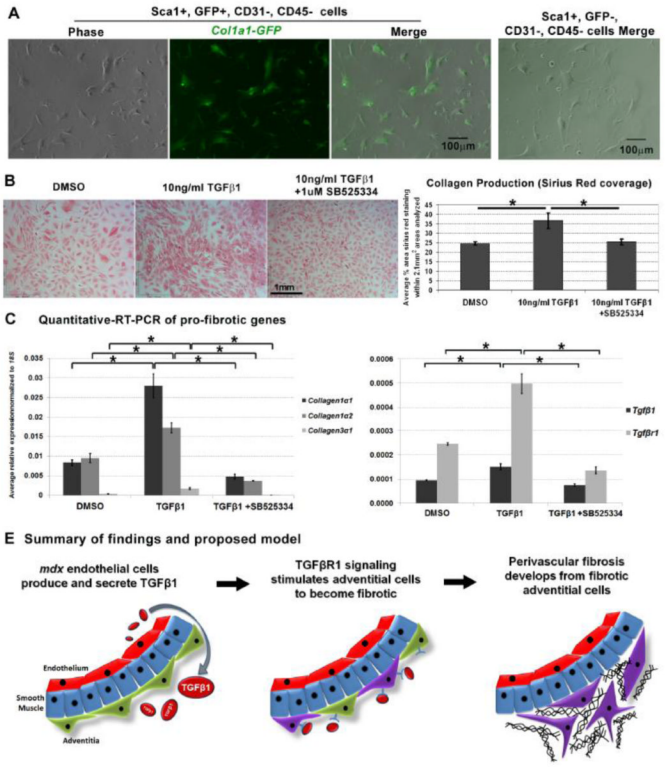

Fig. 6.

Sca1+ adventitial cells maintain expression of *Collagen1α1-GFP* and become fibrotic in response to TGFβ1 stimulation. A. GFP+, Sca1+, CD31−, CD45− cells FACS-sorted from 4 month old wt *Col1α1-GFP* hearts maintained expression of GFP in culture. In contrast, GFP-, Sca1+, CD31−, CD45− cells sorted in parallel never expressed *Collagen1α1-GFP* in culture, right photograph. B. GFP+, Sca1+ sorted cells were treated with the TGFβ1 ligand (10ng/ml) to assess their fibrotic response. In parallel, cells were treated with the vehicle (DMSO) and in conjunction with TGFβ1, an inhibitor of TGFβR1 signaling (SB525334). Each experimental condition was conducted with four replicates (n=4 replicates per condition). Following 4 days of treatment, cells were fixed and stained for collagen with picrosirius red representative photographs that were used for analysis and quantification of collagen production (picrosirius red coverage) with each treatment. Quantification reveals that cells treated with TGFβ1 produced more collagen vs. vehicle controls and cells exposed to 1μM of SB525334. C. In a duplicate experiment, cells were collected for quantitative-RT-PCR analysis of pro-fibrotic genes (n=4 replicates per condition). Analogous to the results in B, cells treated with 10ng/ml TGFβ1 expressed significantly higher levels of *Collagen1α1*, *1α2* and *3α1* as compared to cells treated with DMSO and 10ng/ml TGFβ1 +1μM SB525334. Error bars represent SEM, *P<0.005 derived from Student's *t*-test. D. Model summarizing our results and mechanism of TGFβ1 mediated perivascular fibrosis.